AJNR Am J Neuroradiol 26:662–665, March 2005

Case Report

MR Imaging of Hyperacute Subarachnoid and Intraventricular Hemorrhage at 3T: A Preliminary Report of Gradient Echo T2*-Weighted Sequences

Chul-Ho Sohn, Seung-Kug Baik, Hee-Jung Lee, Sung-Moon Lee, Il-Man Kim, Man-Bin Yim, Jae-Suk Hwang, M. Louis Lauzon, and Robert J. Sevick

Summary: We describe MR imaging findings applying gradient echo (GRE) T2*-weighted and fluid-attenuated inversion recovery (FLAIR) MR images at 3T to three patients with hyperacute subarachnoid and intraventricular hemorrhage from ruptured aneurysms. Hyperacute subarachnoid and intraventricular hemorrhages (SAH and IVH) were more clearly visualized as an area of decreased signal intensity on GRE T2*-weighted sequences than on FLAIR sequences in all three patients. These preliminary results suggest that acute SAH and IVH with GRE T2*-weighted imaging can be reliably diagnosed at 3T.

Previous studies have demonstrated that fluid-attenuated inversion recovery (FLAIR) sequences are very sensitive to acute (<12 hours) subarachnoid hemorrhage (SAH) and acute (<48 hours) intraventricular hemorrhage (IVH) at 1.5T (1, 2). One study described the high accuracy of gradient-echo (GRE) T2*-weighted imaging in the detection of acute (<4 days) SAH at 1.5T (3). We have found no reports of MR imaging findings of hyperacute SAH and IVH on GRE T2*-weighted and FLAIR sequences at 3T. We report the preliminary results of GRE T2*-weighted and FLAIR sequences at 3T applied to three patients with hyperacute SAH and IVH.

Case Reports

We obtained MR images after diagnosing SAH by CT scan. The MR imaging studies were performed by using a whole-body 3T system (Signa VH/i, General Electric, Milwaukee, WI) in three patients within 12 hours (mean 6.9 hours) after the onset of symptoms. The MR imaging protocol consisted of fast FLAIR (TR/TE, 8802/161 ms; inversion time, 2200 ms) and GRE T2*-weighted (TR/TE, 325/20 ms; flip angle, 15) images. Conventional spin-echo (SE) noncontrast T1-weighted images (TR/TE, 600/14 ms) and fast spin-echo (FSE) T2-weighted images (TR/TE, 4500/106.9 ms) were also obtained. The average time gap between CT scan and MR imaging was 3.3 hours.

Case 1

A 65-year-old woman had a sudden-onset headache. CT scan obtained 7.3 hours after the ictus showed SAH in the sylvian fissures and interhemispheric fissure as well as IVH in the 3rd and both lateral ventricles (Fig 1A). FLAIR images obtained 10.3 hours after the ictus showed the SAH as an area of mildly increased signal intensity relative to brain parenchyma and subtle IVH as area of mildly increased signal intensity relative to CSF (Fig 1B). GRE T2*-weighted images clearly showed the SAH and IVH as areas of decreased signal intensity (Fig 1C). FSE T2-weighted images also showed the IVH as area of decreased signal intensity in the lateral and 3rd ventricle but did not visualize the Sylvian SAH (Fig 1D). Preoperative noncontrast time-of-flight (TOF) MR angiography visualized a left anterior communicating artery aneurysm. An external ventricular drain (EVD) was inserted, and the aneurysm was clipped.

Case 2

A 52-year-old woman had a sudden-onset dull headache. A CT scan obtained 1.3 hours after the ictus showed a diffuse SAH and IVH in the 3rd ventricle (Fig 2A). FLAIR images obtained 5.1 hours after ictus showed the SAH as areas of high signal intensity relative to brain parenchyma in the Sylvian cisterns bilaterally but did not show the IVH (Fig 2B). GRE T2*-weighted images showed an obvious SAH and IVH as areas of decreased signal intensity (Fig 2C). Preoperative noncontrast TOF MR angiography demonstrated a left anterior communicating artery aneurysm. The aneurysm was treated surgically.

Case 3

A 47-year-old man had a severe sudden-onset headache. A CT scan obtained 2.5 hours after the ictus showed a SAH in the Sylvian and basal cisterns as well as over the left hemisphere cortical sulci. The IVH was not evident on the CT scan. FLAIR images obtained 5.5 hours after the ictus showed the SAH as area of high signal intensity relative to brain parenchyma in the subarachnoid spaces and the IVH as areas of mildly increased signal intensity relative to CSF in the lateral ventricles. GRE T2*-weighted images revealed decreased signal intensity in the subarachnoid space and ventricle. Preoperative noncontrast TOF MR angiography visualized an aneurysm involving the left M1 segment of the middle cerebral artery. Surgery confirmed the ruptured aneurysm.

Discussion

Recent advances in high-field technology and the increased availability of 3T MR imaging units have

Received February 23, 2004; accepted after revision June 18.

From the Departments of Radiology (C.-H.S., S.-K.B., H.-E.L., S.-M.L.), Neurosurgery (I.-M.K., M.-B.Y.), and Internal Medicine (J.-S.H.), Keimyung University, Daegu, Korea; and the Department of Radiology (C.-H.S., M.L.L., R.J.S.), University of Calgary, and Seaman Family MR Research Centre and Foothills Medical Centre (M.L.L., R.J.S.), Calgary Health Region, Calgary, Alberta, Canada.

Address correspondence to Chul-Ho Sohn, MD, Department of Radiology, Dongsan Medical Center, Keimyung University School of Medicine, 194 DongSan-Dong, Jung-Ku, Daegu 700-712, Korea.

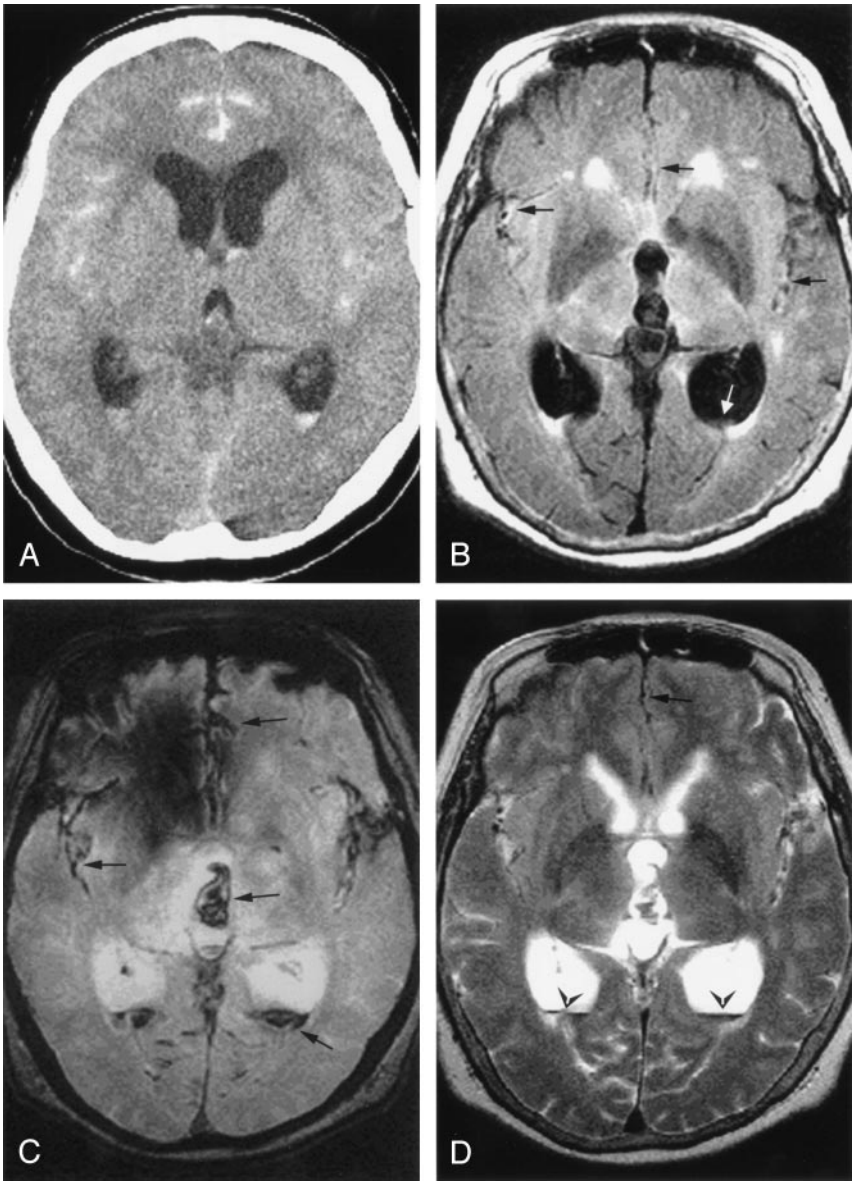

FIG 1. Case 1, a 65-year-old woman with hyperacute SAH and IVH due to a ruptured left anterior communicating artery aneurysm.

A, CT scan (7.3 hours postictus) shows an SAH and IVH in the both Sylvian fissures, the anterior interhemispheric fissure, and the occipital horns of both lateral ventricles.

B–D, MR images obtained 10.3 hours postictus. Axial FLAIR image (*B*) shows high signal intensity in the anterior interhemispheric fissure and both Sylvian fissures (*black arrows*). A layered area mildly increased signal intensity is evident in occipital horn of the left lateral ventricle (*white arrow*). Axial GRE T2*-weighted image (*C*) shows decreased signal intensity in the interhemispheric and both Sylvian fissures, 3rd ventricle, and occipital horns of both lateral ventricles (*arrows*). Axial fast spin-echo T2-weighted image (*D*) shows linear low signal intensity in the anterior interhemispheric fissure (*arrow*) and blood-CSF layered pattern of the IVH (*arrowheads*) in the occipital horns of both lateral ventricles.

opened the possibilities for a variety of exciting improvements in clinical and research applications of MR imaging. At 3T, augmentation of susceptibility effects induces several disadvantages, including a shortening of T2 and T2*, signal intensity loss, and geometric distortion. Associated advantages, however, need to be considered. One example is the increased sensitivity to deoxyhemoglobin-induced susceptibility, which in turn improves the quality of functional MR imaging and the detection of hemorrhage (4).

Hyperacute SAH in patients within 12 hours of symptom onset can be detected by using FLAIR sequences at 1.5 or 1T (1, 5, 6). In these reports, FLAIR images clearly visualized SAHs as area of high signal intensity; however, 66% of hyperacute IVHs were not visualized by using FLAIR images (1). MR findings on FLAIR images in our patients are in accordance with those in the literature, except that the signal intensity of hemorrhage was not greatly increased. The possible cause of different signal intensity of SAHs and IVHs on FLAIR is combination of shortening of T1 and T2* relaxation time at 3T. The markedly shortened T2* may decrease the signal intensity of hemorrhage, compared with 1.5T. Another explanation is long TE of our imaging parameter, which may counteract the hyperintensity of the SAH on FLAIR.

One case of hyperacute SAH and IVH has been reported by using GRE T2*-weighted sequence (7). In this report, hyperacute SAH and IVH were of mildly decreased signal intensity on GRE T2*-weighted images and showed increased signal intensity relative to the CSF on FLAIR and spin-echo T2-weighted images. In our cases, the hyperacute hemorrhage was of very low signal intensity on GRE T2*-weighted images. FSE T2-weighted images showed the IVH as area of decreased signal intensity relative to CSF. These different appearances of hyperacute hemorrhage on MR images may be explained by multiple factors: different field strength;

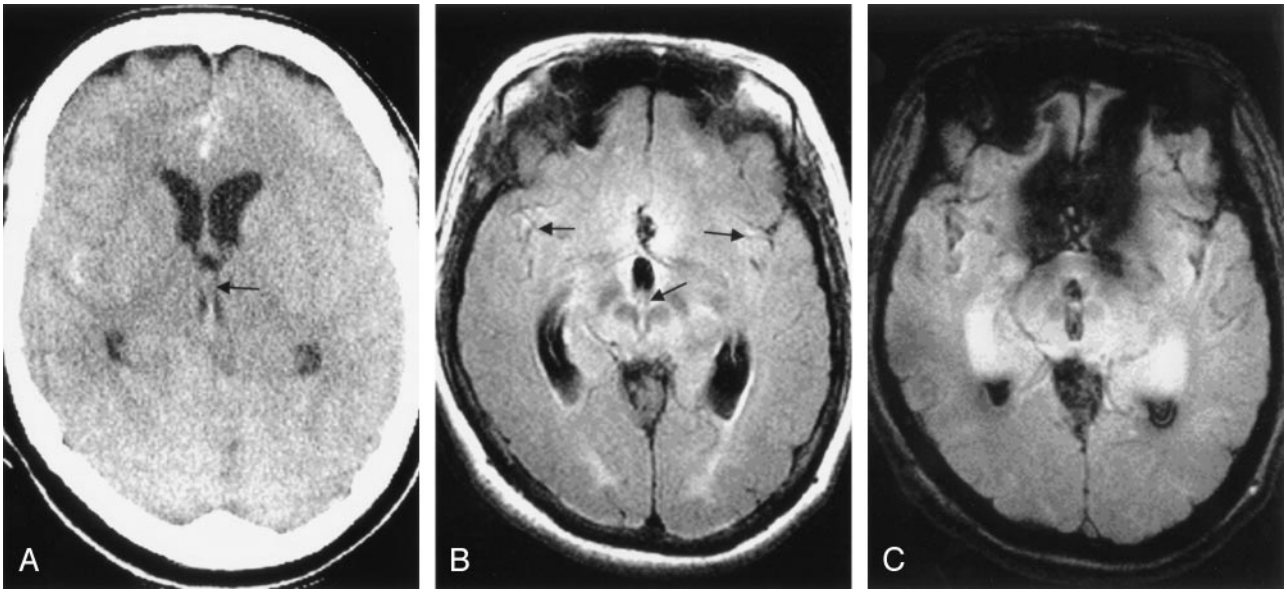

FIG 2. Case 2, a 52-year-old woman with hyperacute SAH and IVH due to a ruptured left anterior communicating artery aneurysm. *A,* CT scan (1.3 hours postictus) shows extensive SAHs and IVHs in the 3rd ventricle (*arrow*). IVH is not evident in the lateral ventricle. *B* and *C,* MR images obtained 5.1 hours postictus. Axial FLAIR image (*B*) shows increased signal intensity in both Sylvian fissures and 3rd ventricle (*arrows*). IVH in lateral ventricle is not visualized. Axial GRE T2*-weighted image (*C*) clearly shows the SAH and IVH in the Sylvian fissures bilaterally as well as 3rd ventricle and occipital horn of both lateral ventricles.

different imaging delay time (<1 hour as opposed to 5.5 hours); hemorrhage pattern, especially IVH layer form (blood-CSF fluid-fluid level). Higher field strength, increased susceptibility effect, and longer MR imaging delay time increase the amount of deoxyhemoglobin. In addition, dependently layered IVH contains more packed RBC clusters. All of these factors increase magnetic susceptibility of deoxyhemoglobin (i.e., shorten T2* and signal intensity loss) in hyperacute hemorrhage on GRE T2* and to a lesser extent on FSE T2-weighted sequences. The augmented signal intensity loss due to deoxyhemoglobin is more readily detected on GRE T2*-sequence. Because FSE T2-weighted sequence has less susceptibility effect than GRE T2*-weighted, a diluted SAH is difficult to visualize by using FSE T2-weighted imaging. One of the limitations of GRE T2*-weighted sequences is that the strong susceptibility artifact at the skull base cannot be reliably distinguished from low signal intensity due to subarachnoid blood.

In addition to FLAIR and GRE sequences, proton-attenuation (PD)–weighted imaging also had high sensitivity to detect SAH (1, 8). Wiesmann et al (1) reported that PD-weighted images had higher sensitivity to detect IVH and were less sensitive to artifact than were FLAIR images. But our study did not include PD-weighted images because they are not routine neuroimaging sequences at our institution.

CT is still widely and most commonly used to exclude intracerebral hemorrhages and SAHs because CT has excellent accessibility, compared with MR imaging, in acutely ill patients. CT-based diagnosis of a SAH may also be difficult in the posterior fossa because of bone artifacts as well as with small amounts of blood. Moreover, MR imaging is also effective in the diagnosis of an acute SAH (1, 6) and diffusion-weighted (DW) images provide additional information of brain damage directly attributable to SAH (9). Accuracy of detection of SAH by using DW imaging is controversial. Wiesmann et al (1) reported that DW imaging could not detect SAH in all 13 SAH cases. Fiebach et al (8), however, reported that DW images visualized SAH as high signal intensity in four of five cases. Thus, further studies aimed at the diagnostic reach of DW imaging in acute SAH are worthwhile.

Conclusion

GRE T2*-weighted sequence at 3T demonstrated hyperacute SAH and IVH areas of decreased signal intensity in our patients. And GRE T2*-weighted images appear to be more sensitive than FLAIR images in the detection of hyperacute SAHs and IVHs at 3T. Our findings in high-grade SAHs (Fisher grade 4), however, may justify further studies in low-grade SAHs that especially are located at the anterior basal and pontine cisterns.

References

1. Wiesmann M, Mayer TE, Yousry I, et al. **Detection of hyperacute subarachnoid hemorrhage of the brain by using magnetic resonance imaging.** *J Neurosurg* 2002;96:684–689
2. Bakshi R, Kamran S, Kinkel PR, et al. **Fluid-attenuated inversion-recovery MR imaging in acute and subacute cerebral intraventricular hemorrhage.** *AJNR Am J Neuroradiol* 1999;20:629–636
3. Mitchell P, Wilkinson ID, Hoggard N, et al. **Detection of subarachnoid haemorrhage with magnetic resonance imaging.** *J Neurol Neurosurg Psychiatry* 2001;70:205–211

4. Lin W, An H, Chen W, et al. **Practical consideration for 3T imaging.** *Magn Reson Imaging Clin North Am* 2003;615–639
5. Kuker W, Thiex R, Block F. **Hyperacute perimesencephalic subarachnoid hemorrhage: demonstration of blood extravasation with MRI.** *J Comput Assist Tomogr* 1999;23:521–523
6. Noguchi K, Ogawa T, Inugami A, et al. **MR of acute subarachnoid hemorrhage: a preliminary report of fluid-attenuated inversion-recovery pulse sequences.** *AJNR Am J Neuroradiol* 1994; 15:1940–1943
7. Rumboldt Z, Kalousek M, Castillo M. **Hyperacute subarachnoid hemorrhage on T2-weighted MR images.** *AJNR Am J Neuroradiol* 2003;24:472–475
8. Fiebach JB, Schellinger PD, Geletneky K, et al. **MRI in acute subarachnoid haemorrhage;findings with a standardised stroke protocol.** *Neuroradiology* 2004;44–48
9. Hadeishi H, Suzuki A, Yasui N, et al. **Diffusion-weighted magnetic resonance imaging in patients with subarachnoid hemorrhage.** *Neurosurgery* 2002;50:741–748